Oxidation of Orthorhombic Titanium Aluminide TI-22AL-25NB in Air between 650 and 1000 °C

C. Leyens

(Submitted 13 January 2000)

The oxidation behavior of orthorhombic titanium aluminide alloy Ti-22Al-25Nb was studied in air between 650 and 1000 °C by isothermal thermogravimetry and postoxidation scanning electron microscopy (SEM), energy dispersive spectroscopy (EDS), and x-ray diffraction. Microhardness measurements were performed after exposure to gage hardening due to nitrogen and oxygen ingress. The parabolic rate constant of Ti-22Al-25Nb was of the same order as conventional titanium alloys and Ti_3Al-based titanium aluminides at and below 750 °C. Between 800 and 1000 °C, the oxidation resistance of Ti-22Al-25Nb was as good as that of γ-TiAl based aluminides; however, the growth rate changed from parabolic to linear after several tens of hours at 900 and 1000 °C. The mixed oxide scale consisted of TiO_2, $AlNbO_4$, and Al_2O_3, with TiO_2 being the dominant oxide phase. Underneath the oxide scale, a nitride-containing layer formed in the temperature range investigated, and at 1000 °C, internal oxidation was observed below this layer. In all cases, oxygen diffused deeply into the subsurface zone and caused severe embrittlement. Microhardness measurements revealed that Ti-22Al-25Nb was hardened in a zone as far as 300 μm below the oxide scale when exposed to air at 900 °C for 500 h. The peak hardness depended on exposure time and reached five times the average hardness of the bulk material under the above conditions.

Keywords Nb effect, nitride, orthorhombic phase, oxidation, oxygen embrittlement, titanium aluminide

1. Introduction

Considerable interest has been placed on titanium alloys based on the orthorhombic phase Ti_2AlNb for lightweight applications in aeroengines.[1] For some orthorhombic alloys, a better fracture toughness, higher ductility, higher specific yield, and lower coefficient of thermal expansion than for γ-TiAl based alloys as well as for alpha-2 alloys had been reported.[2,3] The envisaged maximum use temperature of 650 to 700 °C is somewhat lower than for γ-TiAl based intermetallics. Due to a promising balance of mechanical properties, the class of orthorhombic alloys is also being considered for matrix applications in fiber-reinforced titanium composites intended to meet the future structural material requirements for advanced compressor designs.[2,4,5] Similar to conventional titanium alloys and titanium aluminides, the limited oxidation resistance is of concern for orthorhombic alloys. Experimental evidence[6–10] has shown that titanium alloys and aluminides with an aluminum content roughly below about 50 at.% essentially form nonprotective mixed $TiO_2 + Al_2O_3$ scales in air in the anticipated service temperature range rather than dense protective alumina scales. Orthorhombic alloys with an aluminum content of less than about 25% are also not expected to form protective scales. Furthermore, embrittlement of the alloys by dissolution of interstitials is of concern with orthorhombic alloys. The room-temperature ductility as well as the strength of $\beta + Ti_2AlNb$ titanium aluminide alloy Ti-22Al-23Nb was reported to be sensitive to the presence of surface oxides and oxygen-enriched surface layers.[11] Only a few studies on the environmental behavior of orthorhombic titanium alloys with an Al content on the order of 20 to 25 at.% and a relatively high niobium content are known in the open literature.[4,12–15] Ti-24Al-20Nb and Ti-22Al-20Nb were shown to have poor oxidation resistance as compared with α_2-based Ti-25Al-11Nb and to suffer from extensive scale spallation on isothermal exposure at 800 and 900 °C.[12,13] In 1 h cyclic oxidation tests at 700 and 800 °C, Ti-25Al with niobium additions between 5 and 25% exhibited reasonable environmental resistance up to 1000 cycles only for the lower niobium-containing alloys (5 to 15%).[14] Massive mass gain due to breakaway oxidation was found for the higher niobium contents (20 to 25%) after about 600, 1 h cycles at 700 °C and 100, 1 h cycles at 800 °C.[14]

In the present paper, the oxidation behavior of cast Ti-22Al-25Nb between 650 and 1000 °C in air will be discussed regarding scaling behavior and embrittlement of the alloy underneath the oxide scale.

2. Experimental

Ti-22Al-25Nb (Ti-21.8Al-24.9Nb in at.% with 500 ppm oxygen) was produced by the GfE-Gesellschaft für Elektrometallurgie (Nüremberg, Germany) in cooperation with the DLR-German Aerospace Center, by employing vacuum induction melting. The 60 kg ingot material was triple-melted. Part of the ingot was hot worked by swaging up to 95% total reduction at 960 °C. Solution heat treatment at 1000 °C was performed for 30 min with subsequent air cooling. The phase make-up was ordered $\beta + Ti_2AlNb + \alpha_2$ for the swaged microstructure[15] and sample geometries were o.d. 6×1 mm^2. The sample front sides were ground with 1200 grit SiC paper and the edges were

C. Leyens, DLR-German Aerospace Center, Institute of Materials Research, 51170 Cologne, Germany. Contact e-mail: christoph.leyens@dlr.de.

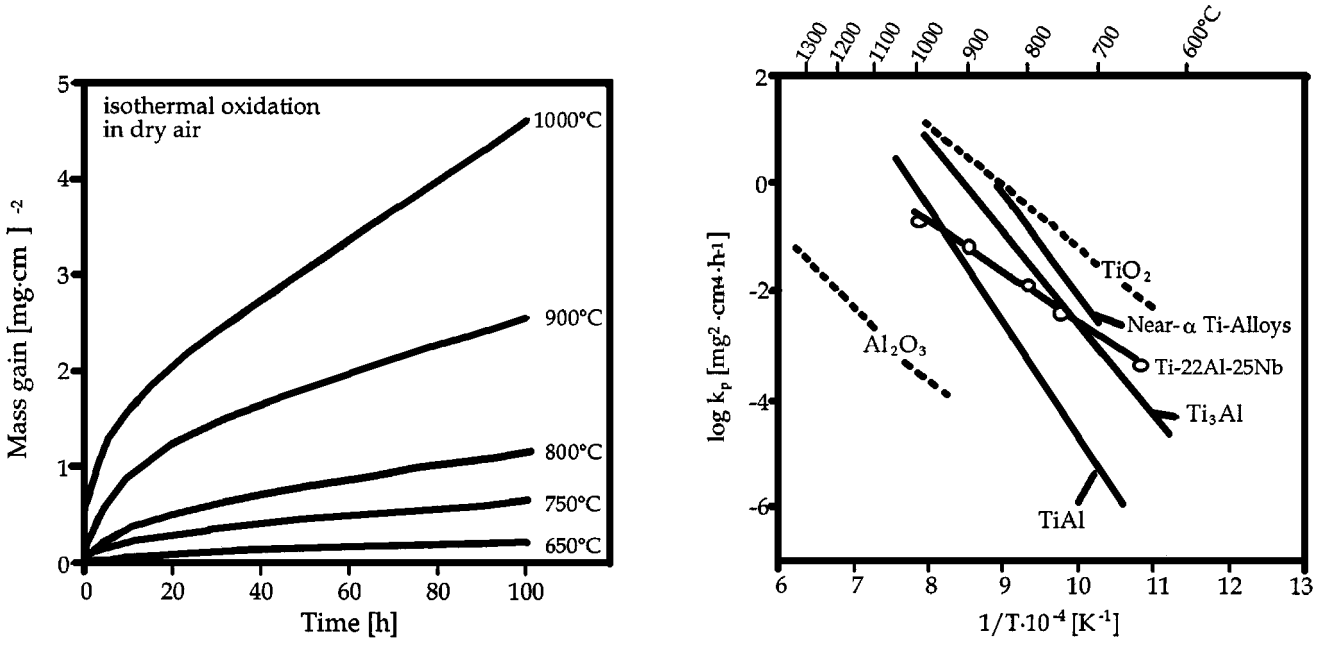

(**a**) (**b**)

Fig. 1 (**a**) Mass gain vs time curves for isothermal oxidation of Ti-22Al-25Nb in air between 650 and 1000 °C up to 100 h. The data indicated linear oxidation rates between 650 and 800 °C and paralinear rates at 900 and 1000 °C. (**b**) The temperature dependency of the parabolic rate constant was significantly different from that of other titanium aluminides and conventional titanium alloys

slightly rounded to minimize stress accumulation. Isothermal oxidation tests in dry air were performed in a Setaram (Caluiere, France) thermobalance between 650 and 1000 °C. The heating rate was 50 K · min^{-1} and the temperature deviation during the tests was smaller than ±0.7 °C. Microhardness measurements to qualitatively study oxygen/nitrogen diffusion were carried out on metallographically polished cross sections using a Vickers indenter under 25 g load applied for 15 s. The diffusion profiles were compared with results of chemical analysis by energy dispersive spectroscopy (EDS). For scanning electron microscopy (SEM) imaging and EDS, a Philips scanning electron microscope 430 (Philips Electronic Instruments Corp., Mahwah, NJ) and a LEO (LEO Electron Microscopy, Ltd., Cambridge, UK) 982 Gemini equipped with a Schottky field emission cathode and an Oxford (Oxford Instruments, Scotts Valley, CA) EDS system were used. The spot size of the electron beam and the excitation area was kept at a very low level, in order to enable proper EDS investigation of thin oxide scales. Formation of oxide phases after oxidation was determined by x-ray diffraction using a Siemens (Siemens, Munich, Germany) D5000 powder diffractometer.

3. Results and Discussion

Mass gain versus time curves for isothermal oxidation of Ti-22Al-25Nb in air at temperatures between 650 and 1000 °C are shown in Fig. 1(a). In the temperature range between 650 and 800 °C, the kinetics obeyed a parabolic rate law for exposure times up to 100 h. At 900 and 1000 °C, parabolic oxidation rates were found in the initial stages of oxidation only, and the rates became linear after 40 and 25 h of exposure, respectively. Unlike for conventional titanium alloys and titanium aluminides Ti_3Al and TiAl, the temperature dependency of the parabolic rate constant for Ti-22Al-25Nb was significantly lower (Fig. 1b). Among other niobium-containing aluminide alloys with an aluminum content on the order of 22 to 25 at.%, high niobium-containing orthorhombic alloy Ti-22Al-25Nb exhibited fairly poor oxidation resistance, although an improvement of the oxidation behavior of binary Ti-25Al was evident (Fig. 2). The oxidation results were in excellent accordance with literature data obtained for Ti-25Al-25Nb. Comparison of the few literature data available indicated that maximum oxidation resistance with titanium aluminides containing about 25 at.% aluminum was obtained with a niobium content on the order of roughly 10 at.%, as reported by Gauer *et al.*[14] for cyclic oxidation at 700 and 800 °C. The compositional range available for maximum oxidation resistance seemed to be slightly wider at lower temperatures. Although a beneficial effect of niobium additions on the oxidation behavior of titanium aluminides had been observed in many cases for γ-TiAl based intermetallics, the mechanism by which this improvement was achieved is still not well understood. Stroosnijder *et al.*[16] and Sunderkötter *et al.*[17] recently summarized the mechanisms proposed to explain the beneficial effect of niobium on the oxidation behavior of γ-TiAl and Ti_3Al alloys:

- formation of a Ti-rich nitride diffusion barrier at the metal/scale interface;
- increase of the Al activity relative to that of Ti in the alloy, thus facilitating the formation of an alumina-rich scale;
- decreasing the metal and/or oxygen transport by niobium enrichment underneath the oxide scale;

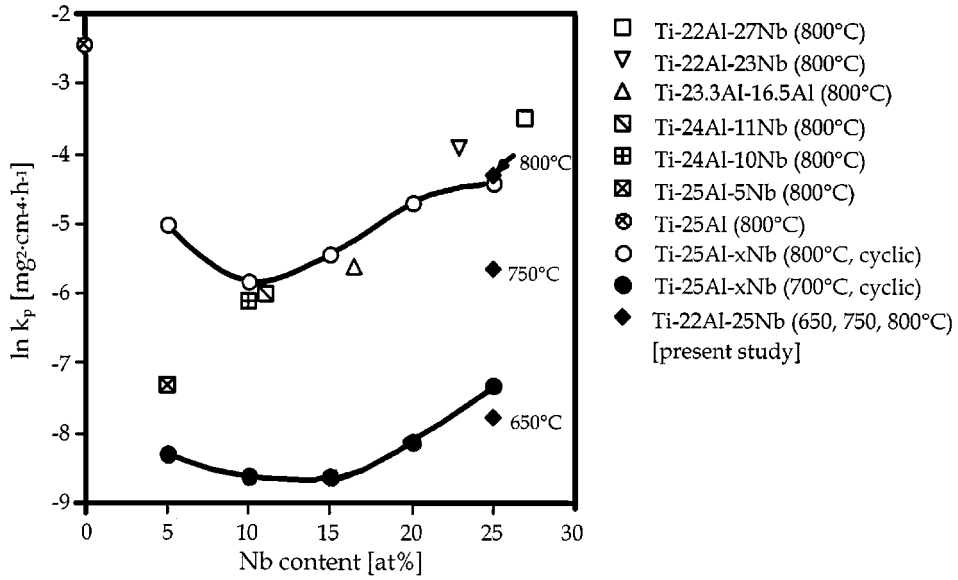

Fig. 2 Parabolic rate constant vs Nb content of various Ti-Al alloys with Al contents between 22 and 25 at.% including Ti-22Al-25Nb. Literature data were obtained from Ref 14 and 20

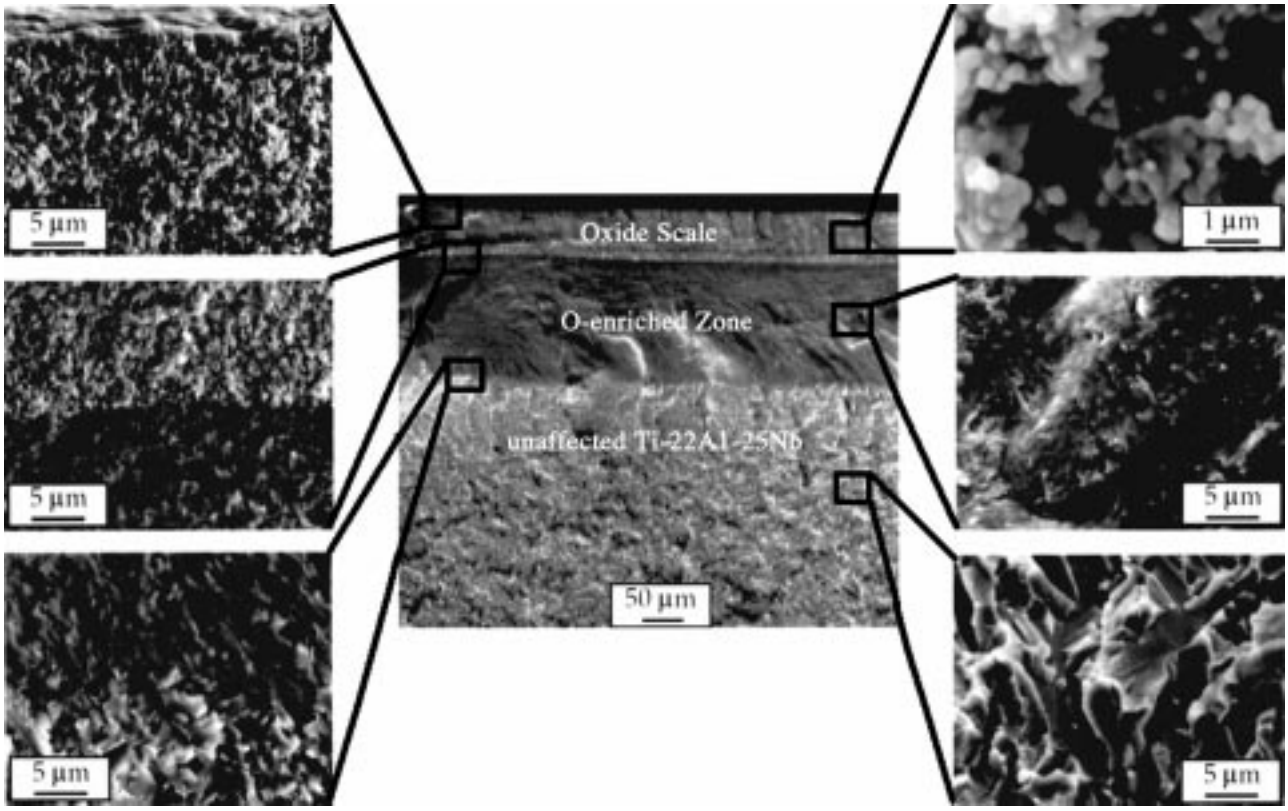

Fig. 3 Fractograph of the oxide scale and the oxygen enriched zone of Ti-22Al-25Nb exposed to air at 900 °C for 500 h. Underneath a fairly dense top oxide layer, a porous oxide scale was found. Below the oxide scale, a 160 μm oxygen-enriched zone formed that fractured brittle

- changing diffusion processes in the scale by doping of the rutile lattice by Nb^{5+} ions;
- formation of Nb_2O_5, thus providing a better bonding between rutile and alumina and blocking rapid diffusion paths; and
- decrease of the oxygen solubility in the alloy.

Taking the different experimental conditions and especially the various alloy chemistries into consideration, it seemed likely that more than one mechanism was involved, leading to the

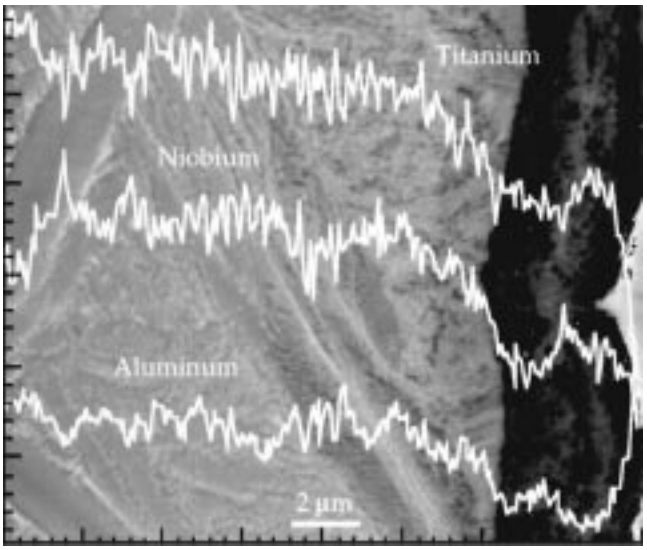

Fig. 4 SEM secondary electron image and EDS linescans of the outer region of Ti-22Al-25Nb isothermally oxidized at 800 °C for 100 h in air

specific experimental findings. The only mechanism to date that was disproved by thoroughly conducted thermodynamic experiments is the effect of Nb on the activity of Al. Vaporization studies on titanium aluminides by Hilpert *et al.*[18] revealed no activity increase of Al relative to the activity of Ti; therefore, Nb additions do not favor the formation of alumina instead of titania.

The oxide scale formed on Ti-22Al-25Nb during exposure between 650 and 1000 °C contained variable amounts of TiO_2, $AlNbO_4$, and Al_2O_3.[15,19] Although the amount of Al_2O_3 in the scale increased with increasing oxidation temperature, TiO_2 was the dominant oxide phase formed in this temperature range. At 900 °C, the surface of the oxide scale was covered with a relatively dense oxide layer, whereas the bulk of the scale consisted of almost spherical oxide particles, which formed a porous scale (Fig. 3). This macroscopic scale make-up was typical of all scales formed between 600 and 1000 °C. Although as thick as 50 μm after 500 h exposure at 900 °C, the oxide scale exhibited excellent adherence. Underneath the oxide scale, an oxygen-enriched zone extended into the alloy that exhibited a brittle fracture morphology, indicating significant alloy embrittlement by dissolution of oxygen (and nitrogen).

Careful SEM/EDS investigation of the metal/scale regions after exposure revealed a microstructurally and chemically layered structure of the oxide scale.[19] After 100 h exposure to air at 800 °C, a 4 μm thick, slightly convoluted oxide scale formed (Fig. 4). The oxide scale consisted of an Al-rich outermost part, followed by Ti- and Nb-enriched layers, as indicated by EDS linescans of the respective elements. As will be shown in more detail in the following discussion, underneath the oxide scale, an oxygen/nitrogen-enriched zone formed during exposure. The chemical scale make-up found after oxidation at 800 °C was representative of the scales formed between 650 and 800 °C.

In contrast to the scales formed at 800 °C, where an Al-rich outer layer was detected, Nb was enriched in the outermost layer along with Al after 100 h exposure at 900 °C (Fig. 5a).

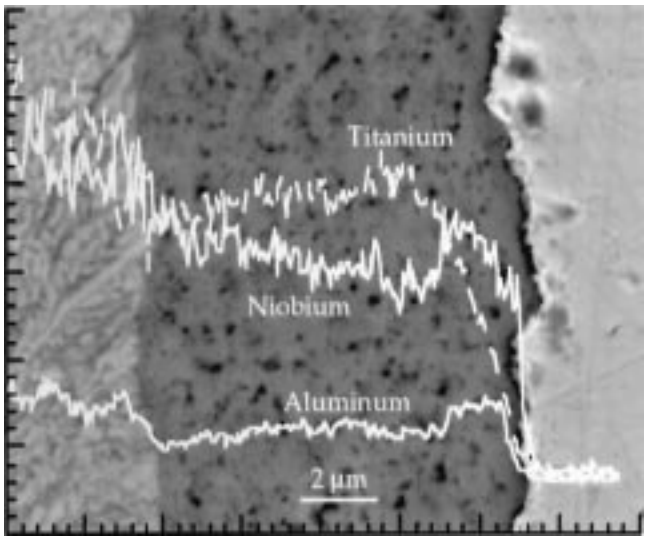

(**a**)

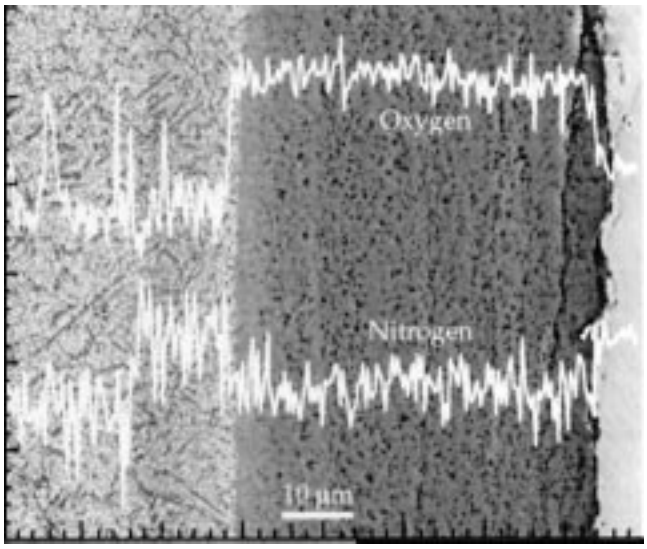

(**b**)

Fig. 5 SEM secondary electron image and EDS linescans of the outer region of Ti-22Al-25Nb isothermally oxidized at 900 °C for 100 h (**a**) and 500 h (**b**) in air. Underneath the oxide scales formed an nitrogen-enriched layer. Nitrogen was probably present as solid solution and as nitrides

The thickness of the nitride-containing layer formed underneath the oxide scale varied from about 1.5 μm after 100 h at 750 °C to about 15 μm after 500 h at 900 °C (Fig. 5b). At a given temperature, the nitride-containing layer grew with increasing exposure time, indicating that nitrogen diffused readily through the growing oxide scale. The nature of the nitrides was not determined; however, both TiN and NbN were the most likely nitride phases to be formed. It should be noted that nitrogen was detected in a fairly limited subsurface zone, whereas oxygen diffused deeper into the alloy. Underneath the nitride-containing layer, the oxygen content was markedly increased compared with the average bulk oxygen level (500 ppm), forming an oxygen diffusion profile into the bulk matrix.

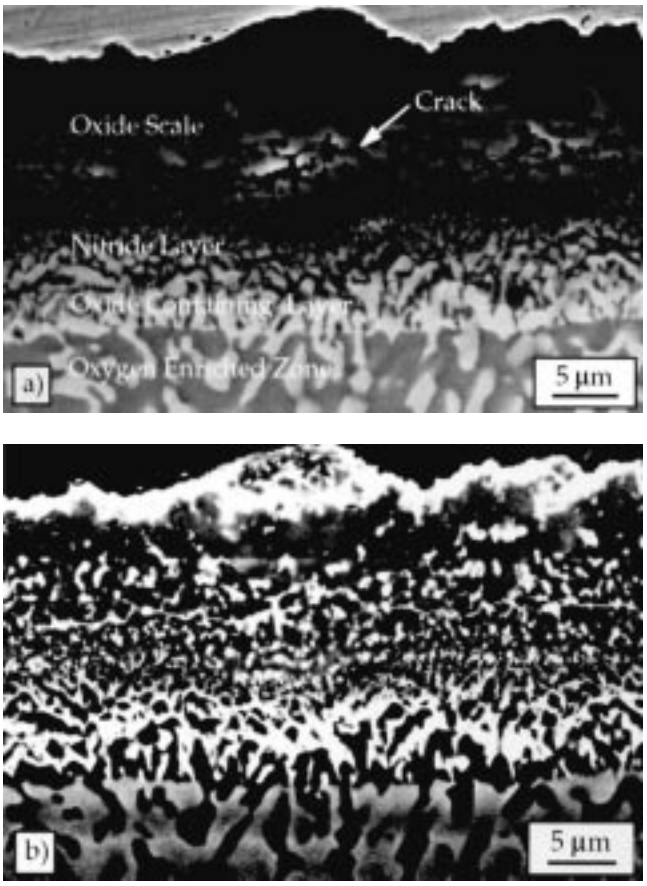

Fig. 6 (**a**) Secondary electron SEM image and (**b**) backscattered electron SEM image of the scale/metal region of Ti-22Al-25Nb after 100 h exposure to air at 1000 °C. Underneath the oxide scale, a nitride-containing layer formed followed by an oxide containing layer and an oxygen-enriched zone. The outermost part of the oxide scale was Nb-rich

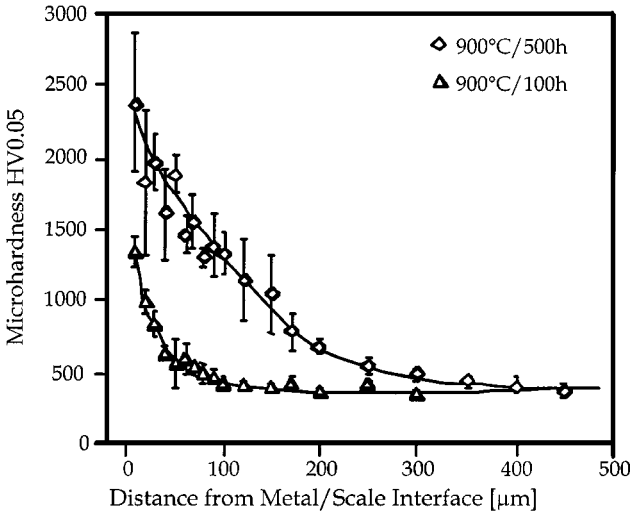

Fig. 7 Microhardness vs distance from the metal/scale interface for Ti-22Al-25Nb exposed to air at 900 °C for 100 and 500 h. Note that the peak hardness was different after both exposure times and that the scatter of data was significantly larger for 500 h exposure

Table 1 Oxygen/nitrogen diffusivities for Ti-22Al-25Nb and Ti-14Al-21Nb[23] in air

Alloy	Temperature/time	D ($m^2\ s^{-1}$)
Ti-22Al-25Nb	800 °C/100 h	$1 \cdot 10^{-15}$
	900 °C/100 h	$2 \cdot 10^{-15}$
	900 °C/500 h	$5 \cdot 10^{-15}$
Ti-14Al-21Nb	800 °C/25 h (1 h)	$0.3 \cdot 10^{-15}$ ($3 \cdot 10^{-15}$)
	900 °C/25 h (1 h)	$1.5 \cdot 10^{-15}$ ($10 \cdot 10^{-15}$)

Figure 6 provides an overview of the layered scale/metal region formed on Ti-22Al-25Nb after 100 h exposure at 1000 °C. Underneath the oxide scale, a nitride-containing layer formed, followed by an oxide-containing layer and finally by an oxygen-enriched zone. Occasionally, internal oxidation occurred in the oxide-containing layer at 900 and 1000 °C. The outermost layer formed at 1000 °C was Nb-rich (Fig. 6b), as were the nitride- and oxide-containing layers. This was in good agreement with findings at 900 °C, where EDS linescans revealed a Nb-rich outer part of the scale (Fig. 5a).

It was well known from earlier work[21] that, from a mechanical perspective, embrittlement of the subsurface of titanium alloys was a major concern regarding alloy applications at elevated temperatures rather than oxide scale formation (and therefore loss of load-bearing cross section) itself. Degradation of mechanical properties (especially ductility) was found to be induced by an oxygen/nitrogen penetration zone. The microhardness profiles for Ti-22Al-25Nb oxidized in air at 900 °C for 100 and 500 h are given in Fig. 7. As expected, the width of the penetration zone increased with increasing exposure time at a given temperature. However, the peak hardness was also significantly higher after longer exposures. Interestingly, the embrittled subsurface zone detected by microhardness measurements was markedly wider (about 300 μm after 500 h at 900 °C) than expected by the extent of brittle fracture morphology (about 160 μm, Fig. 3) found on the same specimen. These results apparently indicated that a certain amount of oxygen/nitrogen dissolution might be tolerable for Ti-22Al-25Nb with respect to the ductility of the alloy. Further mechanical tests are necessary to confirm this assumption.

Microhardness profiles can be used as an indirect measure of oxygen/nitrogen diffusion. According to Roy *et al.*,[22] diffusivities of interstitials in titanium alloys can be calculated by an error function type equation:

$$\frac{MH_1 - MH_0}{MH_2 - MH_0} = \frac{1 - erf\left(\frac{x1}{2\sqrt{Dt}}\right)}{1 - erf\left(\frac{x2}{2\sqrt{Dt}}\right)} \qquad \text{(Eq 1)}$$

For two given points 1 and 2 on the microhardness curve, MH_1 and MH_2 are the respective microhardnesses, and $x1$ and $x2$ represent the respective distances from the alloy/scale interface. MH_0 is the bulk hardness of the alloy, and t is the time of exposure. The diffusion coefficients D for oxygen/nitrogen diffusion in Ti-22Al-25Nb at 800 and 900 °C are listed in Table 1.

Although some of the premises for Eq 1 were not fulfilled for Ti-22Al-25Nb,[19] the agreement with literature diffusivities in Ti-14Al-21Nb was astonishingly good. However, it should be noted that, due to oxidation in air, the coefficients *D* represented the diffusivity of both nitrogen and oxygen.

4. Summary

The isothermal oxidation behavior of Ti-22Al-25Nb was studied in air between 650 and 1000 °C. Although an alumina-rich outer layer formed at temperatures between 650 and 800 °C during exposure, this layer was not fully dense and, therefore, nonprotective due to the presence of TiO_2 and $AlNbO_4$. At higher temperatures, the disappearance of the alumina layer caused a transition of the growth rate from parabolic to linear after short exposure times. Embrittlement of the subsurface zone by nitride layer formation and oxygen/nitrogen penetration was quite remarkable for Ti-22Al-25Nb. After 500 h at 900 °C, the peak hardness at the outermost part of the alloy adjacent to the oxide scale was significantly higher than the bulk hardness. Diffusivities of nitrogen and oxygen calculated from microhardness data were in good agreement with the literature data reported for similar alloys.

Acknowledgments

This work was part of DLR's in-house research activities on orthorhombic titanium aluminide alloys for titanium matrix composite applications. J. Kumpfert at DLR provided the alloy and H. Gedanitz carried out the thermogravimetric experiments. Analytical assistance was given by R. Borath, M. Klaukien, and U. Krebber. M. Peters provided valuable comments on the manuscript.

References

1. J.C. Williams: in *Structural Intermetallics 1997*, M.V. Nathal, R. Darolia, C.T. Liu, P.L. Martin, D.B. Miracle, R. Wagner, and M. Yamaguchi, eds., TMS, Warrendale, PA, 1997, pp. 3-8.
2. J. Kumpfert, M. Peters, and W.A. Kaysser: *Proc. NATO-RTO Symp. on "Design Principles and Methods for Aircraft Engines,"* Toulouse, France, 1998, paper no. 42-1/12.
3. R.G. Rowe: in *Microstructure/Property Relationships in Titanium Aluminides and Their Alloys*, TMS, Warrendale, PA, 1991, pp. 387-98.
4. W.J. Brindley, J.L. Smialek, J.W. Smith, and M.P. Brady: *Proc. 1994 Orthorhombic Titanium Matrix Composite Workshop*, Cincinnati, OH, P.R. Smith, ed., 1994, WL-TR-95-4068, pp. 1-14.
5. S.G. Warrier, S. Krishnamurthy, and P.R. Smith: *Metall. Mater. Trans. A*, 1998, vol. 29A, pp. 1279-88.
6. S. Taniguchi, T. Shibata, and S. Itoh: *JIM*, 1991, vol. 32, pp. 151-56.
7. T.A. Wallace, R.K. Clark, K.E. Wiedemann, and S.N. Sankaran: *Oxid. Met.*, 1992, vol. 37, pp. 111-24.
8. T. Shimizu, T. Ikubo, and S. Isobe: *Mater. Sci. Eng.*, 1992, vol. A153, pp. 602-07.
9. J.S. Fish and D.J. Duquette: *Proc. 3rd Int. Conf. on High Temperature Corrosion and Protection of Materials*, R. Streiff, J. Stringer, R.C. Krutenat, and M. Caillet, eds., Les Editions de Physique, Les Ulix Cedex, France; *J. Phys. IV*, 1993, pp. 411-18.
10. J. Rakowski *et al.*: in *Microscopy of Oxidation II*, S.B. Newcomb and M.J. Bennett, eds., The Institute of Materials, London, 1993, pp. 476-86.
11. F.C. Dary and T.M. Pollock: *Mater. Sci. Eng.*, 1996, vol. A208, pp. 188-202.
12. S.K. Jha, A.S. Khanna, and C.S. Harendranath: *Oxid. Met.*, 1997, vol. 47 (5–6), pp. 465-93.
13. S.K. Jha, A.S. Khanna, and C.S. Harendranath: *Mater. Sci. Forum*, 1997, vol. 251–254, pp. 203-10.
14. L. Gauer, S. Alperine, P. Steinmetz, and A. Vassel: *Oxid. Met.*, 1994, vol. 42 (1–2), pp. 49-74.
15. J. Kumpfert and C. Leyens: *Structural Intermetallics 1997*, TMS, Warrendale, PA, 1997, pp. 895-904.
16. M.F. Stroosnijder *et al.*: *Oxid. Met.*, 1996, vol. 46 (1–2), pp. 19-35.
17. J.D. Sunderkötter, V.A.C. Haanappel, and M.F. Stroosnijder: in *Microscopy of Oxidation III*, S.B. Newcom and J.A. Little, eds., The Institute of Materials, London, 1997, pp. 287-96.
18. K. Hilpert, M. Albers, M. Eckert, and D. Kath: in *Structural Intermetallics 1997*, M.V. Nathal, R. Darolia, C.T. Liu, P.L. Martin, D.B. Miracle, R. Wagner, and M. Yamaguchi, eds., TMS, Warrendale, PA, 1997, pp. 63-71.
19. C. Leyens: *Oxid. Met.*, vol. 52, Nos. 5/6, 1999, pp. 475-503.
20. R.R. Cerchiara, G.H. Meier, and F.S. Pettit: *Proc. 1994 Orthorhombic Titanium Matrix Composites Workshop*, Cincinnati, OH, P.R. Smith, ed., 1994, WL-TR-95-4068, pp. 15-40.
21. C. Leyens, M. Peters, D. Weinem, and W.A. Kaysser: *Metall. Mater. Trans. A*, 1996, vol. 27A, pp. 1709-17.
22. T.K. Roy, R. Balasubramaniam, and A. Ghosh: *Scripta Mater.*, 1996, vol. 34 (9), pp. 1425-30.
23. K.E. Wiedemann, S.N. Sankaran, R.K. Clark, and T.A. Wallace: in *Oxidation of High-Temperature Intermetallics*, T. Grobstein and J. Doychak, eds., TMS, Warrendale, PA, 1989, pp. 195-206.